# MLACA With Modified Grouping Strategy for Efficient Superconducting Circuit Analysis

Ben A. P. Nel and Matthys M. Botha, *Member, IEEE*

***Abstract*—Electromagnetic analysis of superconducting integrated circuits is routinely required for inductance extraction. FastHenry is a well-known, applicable magnetoquasistatic analysis tool. It is accelerated with the multilevel fast multipole algorithm (MLFMA). A multilevel adaptive cross approximation solver with singular value decomposition recompression (MLACA-SVD) was recently proposed for FastHenry, as an alternative to the MLFMA. It was found to be more efficient, with regards to accuracy versus required memory. It uses the same octree grouping as FastHenry's MLFMA. Here, two modified grouping strategies are proposed to further improve MLACA-SVD efficiency by compressing interactions between larger groups, while maintaining scaling performance consistent with valid admissibility of interactions. The strategies are denoted "shell merging" and "wall merging." Results show that the MLACA-SVD solver with merging requires about four times less memory than FastHenry's MLFMA, for similar accuracy. Shell merging is found to be slightly superior.**

***Index Terms*—Group interaction, hierarchical octree, low-rank factorization, partial element equivalent circuit (PEEC), volume integral equation.**

## I. Introduction

INDUCTANCE extraction for superconducting integrated circuits requires the accurate solution of structural current distributions [1]–[4]. This task can be accomplished with FastHenry, which is a well-known, integral equation-based, magnetoquasistatic analysis tool [5]. Storing the entire, dense inductance matrix of dimensions $b \times b$, where $b$ denotes the number of mesh filaments, is prohibitively expensive in computational terms. Therefore, FastHenry uses the multilevel fast multipole algorithm (MLFMA) to compress this matrix. Multilevel adaptive cross approximation with singular value decomposition recompression (MLACA-SVD) was proposed in [6]–[10], for compression of boundary element method (BEM) matrices with asymptotically smooth kernels. Recently, an MLACA-SVD solver was presented as an alternative to the MLFMA, within FastHenry [11]. Results for circuit structures of practical interest show that the MLACA-SVD solver is more efficient than FastHenry's MLFMA. Furthermore, the MLACA-SVD solver offers comprehensive control over the errors introduced by the algorithm. In [11] quadrature recipes of guaranteed accuracy are presented, such that matrix-entry numerical integration error contributions are small enough that overall accuracy is solely determined by the compression tolerance setting. The MLACA-SVD solver compresses off-diagonal matrix blocks representing interactions between groups of observer and source filaments. This is done on each level. Standard, hierarchical, octree grouping for three-dimensional meshes is employed according to [12]. In pursuit of further matrix storage reduction, group merging strategies for compression of larger matrix blocks at a time, are proposed in this paper. Such strategies would be very difficult to realize within an MLFMA solver, while being fairly straightforward for the MLACA-SVD due to its algebraic nature.

Section II reviews the MLACA-SVD solver and provides motivation for the merging of groups, based on the spherically-symmetric nature of the Green's function and the ACA's group interaction admissibility condition. Two group-merging strategies are presented in Sections III and IV, denoted *shell merging* and *wall merging*, respectively. Section V presents numerical results to assess the performance of the modified grouping strategies, for superconducting integrated circuit modeling. Section VI concludes the work.

## II. MLACA-SVD Overview and Motivation for Group Merging

Circuit structures are discretized into hexahedral filaments with constant, axial current densities. Superconductivity is incorporated via the filaments' self resistances [11]. Magnetic coupling is incorporated via the mutual inductance matrix $L$ [5], [11]. A matrix entry representing the coupling between observer (i.e., testing) filament $i$ and source filament $j$, is calculated as

$$L_{ij} = \frac{\mu}{4\pi a_i a_j} \int_{V_i} \int_{V_j} \frac{\hat{\ell}_i \cdot \hat{\ell}_j}{|\boldsymbol{r} - \boldsymbol{r}'|} dV' dV, \tag{1}$$

where $a_i$, $V_i$ and $\hat{\ell}_i$ denote the cross-sectional area, volume, and axial unit vector of filament $i$, respectively. As shown in [11], the axial unit vectors are factorized out from $L$ in a straightforward manner, leaving the *potential matrix* for MLACA-SVD compression. A near-interaction criterion determines if an observer filament group $P$ and source filament group $Q$ on a given level of the octree, are 'near' or 'far'; near interactions are

Manuscript received October 29, 2018; accepted January 23, 2019. Date of publication February 5, 2019; date of current version March 4, 2019. This work was supported in part by the Office of the Director of National Intelligence (ODNI), Intelligence Advanced Research Projects Activity (IARPA), via the U.S. Army Research Office under Grant W911NF-17-1-0120 and in part by the National Research Foundation of South Africa under Grant 96222. *(Corresponding author: Ben A. P. Nel.)*

The authors are with the Department of Electrical and Electronic Engineering, Stellenbosch University, Stellenbosch 7602, South Africa (e-mail: 17762944@sun.ac.za; mmbotha@sun.ac.za).

Color versions of one or more of the figures in this paper are available online at http://ieeexplore.ieee.org.

Digital Object Identifier 10.1109/TASC.2019.2897581

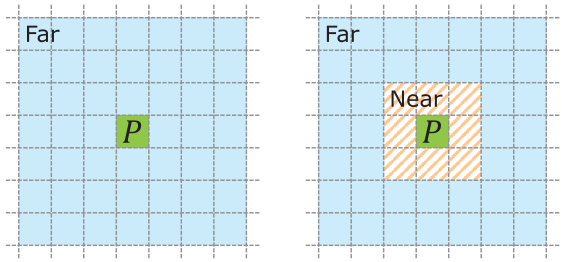


Fig. 1. Two near-interaction criteria, with respect to observer group $P$. Left: self interaction criterion. Right: nearest-neighbor criterion.

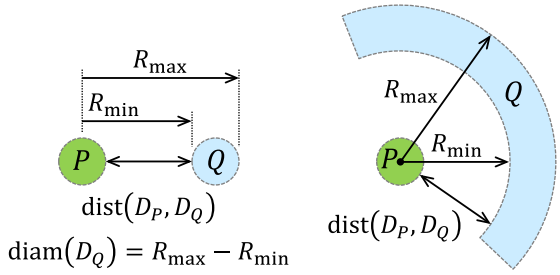


Fig. 2. Left: alternative method of group diameter measurement. Right: set-up with a non-convex source group, for which the alternative $\eta$-admissibility condition is identical to that of the set-up on the left.

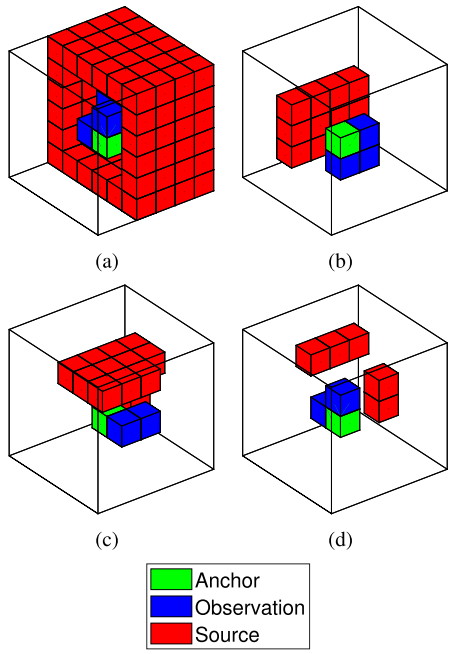


Fig. 3. Shell merging example, which shows the four steps (a) to (d), required in this case to cover all of the anchor's far interactions with source groups. The coloured cubes represent octree groups and the large wire-frame cube depicts the bounding box of all of the anchor's far-interaction source groups. Note that in (a), some of the shared-interaction source groups are not shown for clarity (i.e., a third of the merged "shell" is cut away).

handled down-level, while all far interactions are compressed. Fig. 1 (right) shows the nearest-neighbor criterion used throughout this paper, unless stated otherwise.

The actual suitability for compression of an off-diagonal matrix block representing the coupling between observer group $P$ and source group $Q$, is governed by admissibility conditions. The strong $\eta$-admissibility condition is as follows [6], [13]:

$$\max\{\mathrm{diam}(D_P), \mathrm{diam}(D_Q)\} \leq \eta\, \mathrm{dist}(D_P, D_Q), \quad (2)$$

where $D_P$ and $D_Q$ are the smallest possible, convex hulls enclosing each of the two filament groups. It is required that $\eta > 0$ and be bounded. Fixing the value of $\eta$ limits the extent to which the kernel function $1/|\boldsymbol{r} - \boldsymbol{r}'|$ varies over the two domains. Consequently, it determines the extent of achievable low-rank compression to a given accuracy, for the off-diagonal matrix block; this relates to the nature of exponential decay in the block's singular values.

Now allow for the enclosing domains $D_P$ and $D_Q$ in (2) to be non-convex, together with an alternative way of measuring diameter, namely from the perspective of any given point inside the other domain, as shown in Fig. 2 (left). This yields an alternative $\eta$-admissibility condition. For the set-up in Fig. 2 (left), both the conventional and alternative admissibility conditions yield the same $\eta$ value. However, for the set-up in Fig. 2 (right) the conventional approach yields a dramatically larger (i.e., implied worse) value, while the alternative approach yields the same value as before. The fact that the alternative approach yields equal values, speaks to the kernel function's actual range of variation being equal in both cases, which is due to its spherically-symmetric nature.

The above discussion suggests that a set of observer groups and a set of source groups that are all interacting on a given octree level, could be selected such that the alternative $\eta$-admissibility condition for the two merged groups is fairly similar to those of the individual interactions. Thus, minimized increases in the alternative $\eta$ values, which are expected to minimally reduce compression efficiency, can be traded for compressing larger matrix blocks, which is generally beneficial. Two practical merging strategies are presented next.

## III. Shell Merging

In both merging strategies, each group on a given octree level is considered as observer in turn, to compress all of its far interactions with source groups as well as some of its neighbors' interactions with some of these same source groups. The last observer is not considered, since by definition its interactions would have already been dealt with. For merging purposes the observer group under current consideration is labelled the *anchor group*.

Shell merging is explained with the aid of the example in Fig. 3. Starting with a given anchor, three of its direct neighbors (sharing at least a vertex with it) are sought, such that these neighbors each also shares at least a vertex with one of the others, to ensure a tight cluster with minimized diameter. This yields a merged observer group consisting of four octree groups. The set of far-interaction source groups that are shared by all four observer groups, which can sometimes resemble a shell around the observer cluster, is then identified as shown in Fig. 3(a).

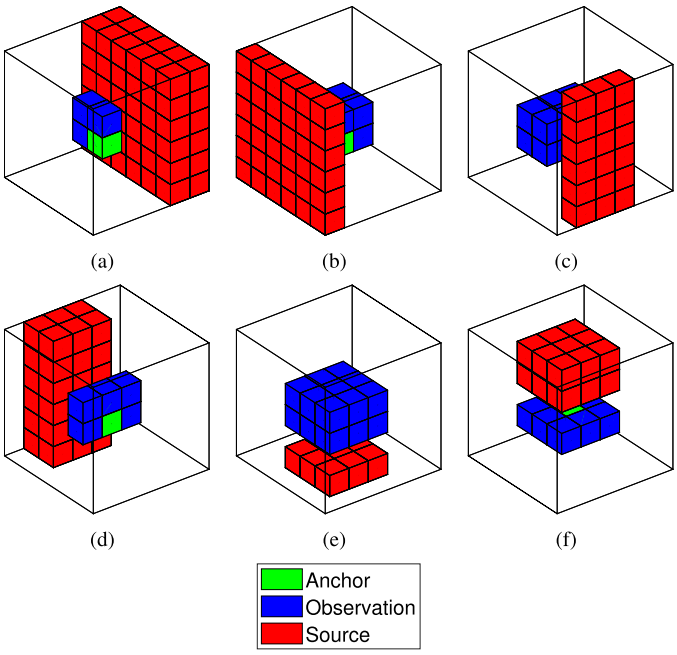


Fig. 4. Wall merging example, which shows the six steps (a) to (f), required to cover all of the anchor's far interactions with source groups. The coloured cubes represent octree groups and the large wire-frame cube depicts the bounding box of all of the anchor's far-interaction source groups.

These source groups are merged and the interaction between merged observer and source groups is compressed with ACA-SVD. Next, three other anchor neighbors are sought according to the same procedure, and the process is repeated, as shown in Fig. 3(b). If there are not enough neighbors left or if three with any shared source interactions cannot be found, then two neighbors are sought instead, as shown in Figs 3(c) and 3(d). These may now include some nearest neighbors previously merged into observer clusters of four, since the condition of shared source interactions is different when the observer cluster is smaller. In the case of the example, all anchor interactions were covered after four steps. In general, the process can progress to seeking only a single neighbor to merge with the anchor; and ultimately to compress the interaction between the anchor on its own, with the merged set of all its remaining far-interaction source groups.

Note that as more and more anchors are processed, less merging opportunities will remain and consequently the large merges shown in the example of Fig. 3 become more scarce.

Finally, the starting goal of merging four observers (rather than a higher number) is chosen for two reasons: it ensures a fair chance that these observers have many far interactions with common source groups, especially when all observers belong to the same octree parent; and it ensures that the merged group diameter is not too large, which would increase $\eta$.

## IV. Wall Merging

Wall merging entails a fixed number of six steps for each anchor group, as shown by the example in Fig. 4. The anchor group's far-interaction source groups are divided into six merged clusters, for compression. Each cluster relates to a face of the anchor group's cubic shape. A cluster is obtained as all of the

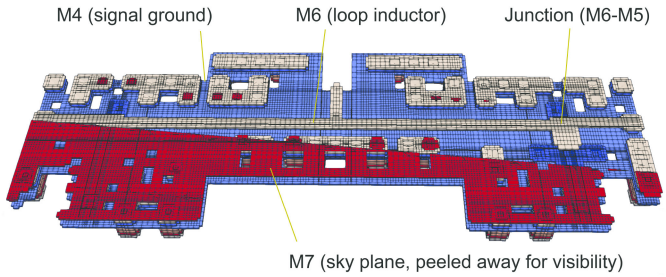


Fig. 5. Test model representing an inductance test SQUID for experimental measurements, with loop inductance in M6 sandwiched between a ground plane in M4 and a ground-connected sky plane in M7 [15].

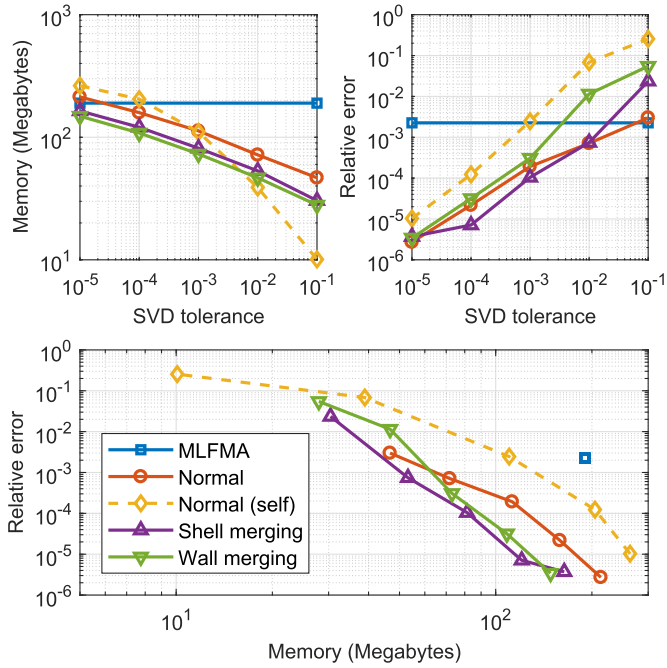


Fig. 6. Memory required to store the mutual inductance matrix (top left) and relative error in the solution port currents (top right). Both quantities are shown as functions of the matrix compression error tolerance $\varepsilon_{\mathrm{SVD}}$, for a mesh of 24,272 filaments. At the bottom, the relative error is shown as a function of memory.

anchor's remaining far-interaction source groups, which lie beyond a flat plane associated with a face. This plane is defined to be parallel to the face and placed at a normal distance of one group side-length away from the face. The source cluster can resemble a wall, as shown in Figs 4(a) to 4(f). Observer groups to be merged with the anchor, are determined as all of its direct neighbors which must still interact with the whole of the merged source. The merged observer cluster sometimes also resembles a wall. Note that unlike with shell merging, it can happen with wall merging that the same merged observation cluster is used multiple times. As with shell merging, fewer merging opportunities will remain as the number of processed anchors increase.

## V. Results

Fig. 5, generated using InductEx [14], shows the superconducting integrated circuit test model [15], which represents an inductance test SQUID. It is meshed with varying filament numbers to obtain all of the results.

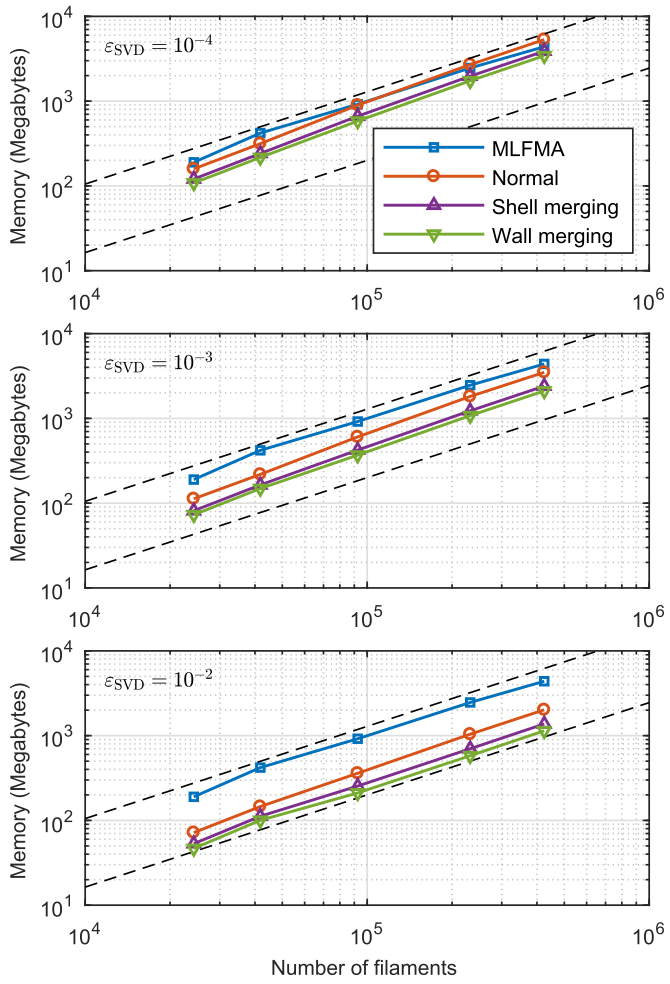


Fig. 7. Memory required to store the mutual inductance matrix, versus number of filaments $b$. The dashed trend lines indicate $\mathcal{O}(b \log b)$ scaling. Top: results with $\varepsilon_{\mathrm{SVD}} = 10^{-4}$. Middle: results with $\varepsilon_{\mathrm{SVD}} = 10^{-3}$. Bottom: results with $\varepsilon_{\mathrm{SVD}} = 10^{-2}$.

Consider a fixed mesh with 24,272 filaments. The SVD error tolerance $\varepsilon_{\mathrm{SVD}}$, which controls the MLACA-SVD matrix compression error [11], is varied. Fig. 6 compares the normal MLACA-SVD, shell-merging MLACA-SVD and wall-merging MLACA-SVD, with FastHenry's MLFMA (the latter gives fixed results, because $\varepsilon_{\mathrm{SVD}}$ is not relevant to it). Observe in Fig. 6 (top left) that the normal MLACA-SVD's dependence of memory requirement upon the logarithm of $1/\varepsilon_{\mathrm{SVD}}$ is preserved by the merging versions. For a fixed value of $\varepsilon_{\mathrm{SVD}}$, both merging versions yield a fixed reduction in required memory of approximately $30\%$, with wall merging being slightly superior. A fifth trace is also shown, for normal MLACA-SVD with the self near-interaction criterion of Fig. 1 (left). This criterion implies $\eta = \infty$ in (2), which is not a valid condition. Its memory scaling is dramatically poorer than the others. The inclusion of this poor result serves to emphasize that the two merging strategies are consistent with maintained admissibility. The solution accuracy results shown in Fig. 6 (top right) are the relative errors in the port currents, as defined in [11]. These results show that convergence towards the true mutual inductance matrix as compression tolerance is decreased, is fairly similar for the normal MLACA-SVD and the two merging versions, especially for $\varepsilon_{\mathrm{SVD}} \leq 10^{-3}$. For a fixed value of $\varepsilon_{\mathrm{SVD}}$, shell merging generally yields superior accuracy to wall merging, which is ascribed to the geometric properties of the former (see Fig. 3) more closely adhering to the idea of maintained (alternative) admissibility as expressed in Fig. 2. Fig. 6 (bottom) combines the two result sets. This shows that for the problem at hand, shell merging is slightly more efficient than wall merging and that both are more efficient than normal MLACA-SVD. All MLACA-SVD versions outperform FastHenry's MLFMA.

Now consider memory scaling with respect to the number of filaments, as shown in Fig. 7. The merging versions scale exactly like the normal MLACA-SVD. Furthermore, the reduction by approximately 30% relative to the normal MLACA-SVD is affirmed for both merging versions, with wall merging again being slightly superior when only memory is considered. Note that for $\varepsilon_{\mathrm{SVD}} = 10^{-2}$, where the merging versions yield compression accuracies similar to FastHenry's MLFMA, the memory requirement is less by about a factor of four.

## VI. Conclusion

With the objective of efficient electromagnetic analysis of superconducting integrated circuits, an MLACA-SVD solver was recently presented for the well-known FastHenry package [11]. It was found to be more efficient than FastHenry's MLFMA solver, with regards to accuracy versus required memory. In this paper, group merging is introduced as a method to further improve the efficiency of this MLACA-SVD solver. Motivation for the concept of merging is provided on the basis of $\eta$-admissibility considerations. Two group merging strategies are proposed. Taking the analysis of a SQUID as an example, numerical results show that both merging strategies yield results consistent with valid admissibility. They reduce the required memory of the MLACA-SVD by approximately $30\%$. Shell merging is marginally more efficient than wall merging, with regards to accuracy versus required memory. For results of similar accuracy as FastHenry's MLFMA, the MLACA-SVD solver with merging requires about four times less memory. For general volumetric structures, rather than the planar integrated circuits of interest here, merging could possibly yield even larger memory reductions due to more opportunities for it. These merging strategies could be tested for other ACA solvers featuring the dynamic kernel, e.g., [16].

## Acknowledgment

The views and conclusions contained herein are those of the authors and should not be interpreted as necessarily representing the official policies or endorsements, either expressed or implied, of the ODNI, IARPA, or the U.S. Government. The U.S. Government is authorized to reproduce and distribute reprints for Governmental purposes notwithstanding any copyright notation herein.

## REFERENCES


[1] P. I. Bunyk and S. V. Rylov, "Automated calculation of mutual inductance matrices of multilayer superconductor intergrated circuits," in *Proc. Extended Abstr. Int. Supercond. Electron. Conf.*, 1993, p. 62.

[2] M. M. Khapaev, A. Y. Kidiyarova-Shevchenko, P. Magnelind, and M. Y. Kupriyanov, "3D-MLSI: Software package for inductance calculation in multilayer superconducting integrated circuits," *IEEE Trans. Appl. Supercond.*, vol. 11, no. 1, pp. 1090–1093, Mar. 2001.

[3] M. Khapaev, M. Y. Kupriyanov, E. Goldobin, and M. Siegel, "Current distribution simulation for superconducting multi-layered structures," *Superconductor Sci. Technol.*, vol. 16, no. 1, pp. 24–27, 2002.

[4] K. Jackman and C. J. Fourie, "Tetrahedral modeling method for inductance extraction of complex 3-D superconducting structures," *IEEE Trans. Appl. Supercond.*, vol. 26, no. 3, Apr. 2016, Art. no. 0602305.

[5] M. Kamon, J. K. White, and M. J. Tsuk, "FASTHENRY: A multipole-accelerated 3-D inductance extraction program," *IEEE Trans. Microw. Theory Techn.*, vol. 42, no. 9, pp. 1750–1758, Sep. 1994.

[6] M. Bebendorf, "Approximation of boundary element matrices," *Numerische Mathematik*, vol. 86, no. 4, pp. 565–589, 2000.

[7] S. Kurz, O. Rain, and S. Rjasanow, "The adaptive cross-approximation technique for the 3-D boundary-element method," *IEEE Trans. Magn.*, vol. 38, no. 2, pp. 421–424, Mar. 2002.

[8] M. Bebendorf and S. Rjasanow, "Adaptive low-rank approximation of collocation matrices," *Computing*, vol. 70, no. 1, pp. 1–24, 2003.

[9] L. Grasedyck, "Adaptive recompression of $\mathcal{H}$-matrices for BEM," *Computing*, vol. 74, no. 3, pp. 205–223, 2005.

[10] M. Bebendorf and S. Kunis, "Recompression techniques for adaptive cross approximation," *J. Integral Equ. Appl.*, vol. 21, no. 3, pp. 331–357, 2009.

[11] B. A. P. Nel and M. M. Botha, "An efficient MLACA-SVD solver for superconducting integrated circuit analysis," accepted for publication in *IEEE Trans. Appl. Supercond.*

[12] K. Nabors and J. White, "FastCap: A multipole accelerated 3-D capacitance extraction program," *IEEE Trans. Comput.-Aided Des. Integr. Circuits Syst.*, vol. 10, no. 11, pp. 1447–1459, Nov. 1991.

[13] L. Grasedyck and W. Hackbusch, "Construction and arithmetics of $\mathcal{H}$-matrices," *Computing*, vol. 70, no. 4, pp. 295–334, 2003.

[14] C. J. Fourie, InductEx, Stellenbosch Univ., Stellenbosch, South Africa, 2018. [Online]. Available: http://www.inductex.info

[15] C. J. Fourie, C. Shawawreh, I. V. Vernik, and T. V. Filippov, "High-accuracy InductEx calibration sets for MIT-LL SFQ4ee and SFQ5ee processes," *IEEE Trans. Appl. Supercond.*, vol. 27, no. 2, Mar. 2017, Art. no. 1300805.

[16] K. Zhao, M. N. Vouvakis, and J. F. Lee, "The adaptive cross approximation algorithm for accelerated method of moments computations of EMC problems," *IEEE Trans. Electromagn. Compat.*, vol. 47, no. 4, pp. 763–773, Nov. 2005.